RESEARCH ARTICLE

J Anim Sci Technol 2024;66(6):1109-1126
https://doi.org/10.5187/jast.2023.e137

JAST
Journal of Animal Science and Technology
pISSN 2672-0191 eISSN 2055-0391

Long noncoding RNA network for lncRNA-mRNA interactions throughout swine estrous cycle reveals developmental and hormonal regulations in reproductive tissues

Yoon-Been Park, Chiwoong Lim, Byeonghwi Lim, Jun-Mo Kim*

Functional Genomics & Bioinformatics Laboratory, Department of Animal Science and Technology, Chung-Ang University, Anseong 17546, Korea

Received: Oct 25, 2023
Revised: Dec 13, 2023
Accepted: Dec 13, 2023

***Corresponding author**
Jun-Mo Kim
Functional Genomics & Bioinformatics Laboratory, Department of Animal Science and Technology, Chung-Ang University, Anseong 17546, Korea.
Tel: +82-31-670-3263
E-mail: junmokim@cau.ac.kr

ORCID
Yoon-Been Park
https://orcid.org/0000-0002-3872-0519
Chiwoong Lim
https://orcid.org/0000-0002-6272-4464
Byeonghwi Lim
https://orcid.org/0000-0001-8489-0044
Jun-Mo Kim
https://orcid.org/0000-0002-6934-398X

Competing interests
No potential conflict of interest relevant to this article was reported.

Funding sources
This work was supported by Korea Institute of Planning and Evaluation

Abstract

The mechanism of estrous cycles of pigs should be explored because their reproductive traits are useful for manipulating productivity and solving problems such as infertility. These estrous cycles should be elucidated to understand the complex interactions between various reproductive tissues (including the ovary, oviduct, and endometrium) and the complex range of hormone secretions during estrous cycles. Long non-coding RNAs (lncRNAs) regulate target genes at transcriptional, post-transcriptional, and post-translational regulation levels in various species. However, unlike mRNAs, lncRNAs in pigs have not been sufficiently annotated, and understanding the protein level of coding genes has limitations in determining the mechanism of the reproductive traits of porcine. In this study, the lncRNAs of the porcine ovary, oviduct, and endometrium were investigated on days 0, 3, 6, 9, 12, 15, and 18 of the estrous cycle. In addition, the characteristics and functions of the identified lncRNAs were explored. 19,021 novel lncRNA transcripts were selected, and the comparison of the characteristics of the newly identified lncRNA and mRNA showed that similar to those of previous studies. Four lncRNA networks were chosen through network analysis. The *cis*-acting genes of lncRNAs included in each network were identified, and expression patterns were compared. The main lncRNAs (XLOC_021792, XLOC_017111, ENSSSCG00000050977, XLOC_000342, ENSSSCG00000050380, ENSSSCG00000045111, XLOC_008338, XLOC_004128, and ENSSSCG00000040267) were determined from the network by considering the *cis*-acting genes. Specific novel lncRNAs were discovered in the reproductive tissues during the swine estrous cycle, and their time-serial expression dynamics were confirmed. As the main lncRNAs are involved in the development of each reproductive tissue and hormone action, they can be utilized as potential biomarkers to help improve and develop the reproductive traits of pigs.

Keywords: Pig, Estrous cycle, Reproductive tissues, RNA-seq, lncRNA

for Technology in Food, Agriculture and Forestry (IPET) through Animal Disease Management Technology Development Program (or Project), funded by Ministry of Agriculture, Food and Rural Affairs (MAFRA) (IPET122005021WT011).
This research was supported by the Chung-Ang University Research Scholarship Grants in 2022.

Acknowledgements
Not applicable.

Availability of data and material
All raw RNA-seq data were deposited at the NCBI Gene Expression Omnibus (http://www.ncbi.nlm.nih.gov/geo/) under the accession number GSE108570.

Authors' contributions
Conceptualization: Park YB, Kim JM.
Data curation: Kim JM.
Formal analysis: Park YB, Lim B.
Methodology: Park YB, Lim C.
Software: Park YB.
Investigation: Lim C, Lim B.
Writing - original draft: Park YB.
Writing - review & editing: Park YB, Lim C, Lim B, Kim JM.

Ethics approval and consent to participate
This article does not require IRB/IACUC approval because there are no human and animal experiments.

INTRODUCTION

The porcine reproductive trait is one of the most important factors in the competitiveness and efficiency of the pig industry, and the reproductive trait of female pigs in particular is directly related to porcine reproductive efficiency [1,2]. The reproductive efficiency in female pigs remarkably affects the litter size, fertility, and hormonal metabolism of pigs [3–5]. Various hormones interacting with one another according to the estrous cycle in turn influence reproductive efficiency [6–8]. Since hormones are secreted and regulated by several reproductive tissues during the estrous cycle, porcine reproductive efficiency is closely associated with molecular mechanisms involved in pig reproductive tissues [9]. Among these reproductive tissues, the ovaries are important because they are a source of reproductive hormones and follicles [10]. They also respond to vital hormones secreted by other organs, especially the pituitary gland, which produces major steroid hormones (estradiol [E4] and progesterone [P2]) and peptide growth factors implicated in the functioning of the ovaries [9,11]. In addition, the oviduct carries follicles from the ovary to the uterus, and its metabolites are affected by ovarian hormones such as E4 and P2 [12,13]. The follicles that ovulate from the ovary move through the oviduct into the uterus. The endometrium is an inner wall of the uterus that prepares for implantation through morphological and functional changes; it also communicates with the ovary through the secretion of prostaglandin F2α (PGF2α) [6,14,15]. Despite relevant studies, the interaction and hormone control mechanisms of reproductive tissues according to the estrous cycle remain difficult and complex. Previous studies showed that a co-expression network can be integrated using whole transcriptomes in each tissue [16,17] and multiple reproductive tissues [6,16,17], but the synchronized interaction of pig reproductive tissues according to the estrous cycle is still insufficient because it is too complicated to be identified only via analysis at the mRNA level.

With the development of next generation sequencing (NGS) technology, noncoding RNAs, which occupy much more areas but do not encode proteins, can be examined [18]. Among noncoding RNAs, long noncoding RNAs (lncRNAs) with a length of 200 bp or more have lower gene expression levels than protein-coding genes, but genes are regulated through transcriptive regulation, post-transcriptive regulation, and RNA interference [19–22]. Most lncRNAs are located in the chromatin and can interact with proteins to promote or inhibit DNA activity in the target DNA region [23]. Therefore, lncRNAs play an important role in genome studies, such as those focusing on mRNA regulation; their characterization in the animal genome can be a key to bridging the gap between genotypes and phenotypes [24]. In addition, the importance of lncRNA is being studied in the fields of infectious diseases, immunity, and pathology; it is considered an important factor in stress response and development regulation in animals [7,25,26]. Thus, lncRNAs have crucial roles in tissue- and species-specific regulation of biological processes (BP) in various species and tissues [27–30]. Currently, studies involving lncRNA analysis have been conducted in pig reproductive tissues, but only a few have explored a single tissue (ovary, oviduct, endometrium) [7,14,31].

Multi-omics analyses have been conducted to obtain complex BP holistically [32,33], and lncRNAs have been considered as a factor for such integrated analysis [34]. The limitations of mRNA-level analysis can be complemented by analyzing the mechanism by which lncRNA manipulates mRNA. In this study, candidate novel lncRNAs were determined, and novel and known lncRNA expression patterns were explored via RNA-seq in three reproductive tissues (ovary, oviduct, and endometrium) throughout the porcine estrous cycle. Significant lncRNA–mRNA pairs were determined to identify tissue- and period-specific lncRNA and mRNA expression and to construct the main lncRNA networks. This study was conducted to confirm the characteristics of lncRNAs according to estrous cycle and reproductive tissues and identify the relationship between

https://doi.org/10.5187/jast.2023.e137

lncRNAs and mRNAs by verifying the regulatory mechanisms of lncRNAs to mRNAs.

METHOD AND METHODS

Ethics, sampling, and sequencing

All animal experimental procedures were approved by the Institutional Animal Care and Use Committee of the National Institute of Animal Science, Republic of Korea (No. 2015-137) and conducted following the Guide for Care and Use of Animals in Research.

Twenty-one crossbred (Landrace × Yorkshire) gilts (age = 6–8 months; weight = 100–120 kg) that underwent at least two normal estrous cycles were used in this study. Three reproductive tissues (ovary, oviduct, and endometrium) of the gilts were collected for sequencing (Fig. 1) on days 0 (designated as the first day of detection of estrous behavior; D00), 3 (D03), 6 (D06), 9 (D09), 12 (D12), 15 (D15), and 18 (D18).

Total RNA was extracted from all reproductive tissues by using TRIzol reagent (Invitrogen, Life Technology, Carlsbad, CA, USA). RNA integrity was evaluated through electrophoresis in 1% agarose gel, and RNA quantity was verified using a NanoDrop ND-1000 spectrophotometer (NanoDrop Technologies, Wilmington, DE, USA). Individual libraries were prepared using an Illumina TruSeq RNA sample preparation kit, and sequencing was performed using cDNA libraries constructed via the 100-base pair (bp) pair-end method in llumina HiSeq 2000. All raw RNA-seq data were deposited at the NCBI Gene Expression Omnibus (https://www.ncbi.nlm.nih.gov/geo/) under the accession number GSE108570. Relevant information was described in detail in our previous study [6,16].

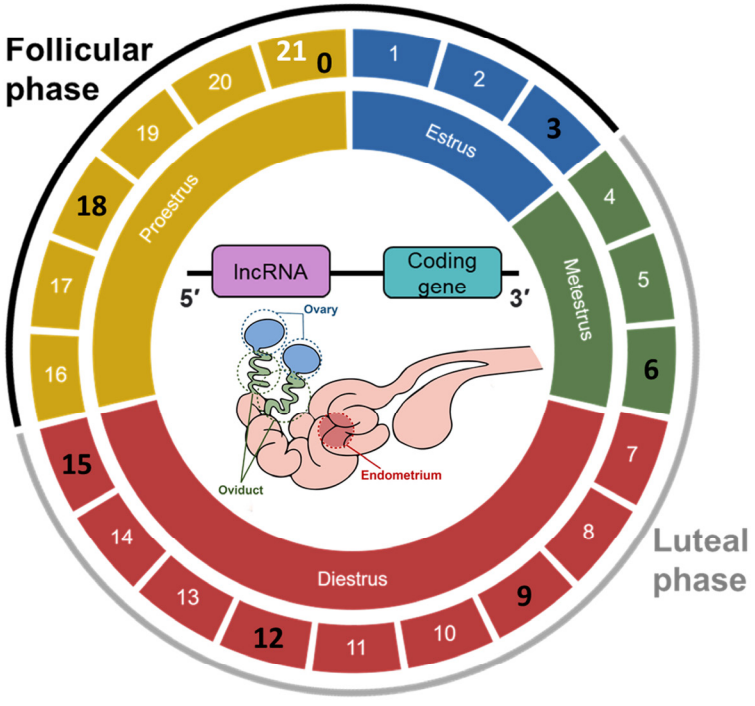

Fig. 1. Overview of three reproductive tissue transcriptomes (lncRNA, coding gene) throughout the estrous cycle. The number of samples (n = 3) in swine reproductive tissue at seven time points (D00, D03, D06, D09, D12, D15, and D18) on the stages of the estrous cycle. lncRNA, long non-coding RNA.

Computational identification of lncRNAs

FastQC software (v.0.11.8) was used to check the quality of raw reads of each sample. For quality control, the reads were processed using Trimmomatic software (v0.39), which removes adaptors and low-quality reads. Hisat2 (v2.1.0) was utilized to map clean reads to the reference genome (Sus scrofa Sscrofa 11.1.99, GCA_000003025.6) of the Ensembl genome browser (http://www.ensembl.org/Sus_scrofa/) as a basis for vsubsequent StringTie application. Samtools (v1.9) was also used to sort the reads mapped in accordance with the criteria for subsequent StringTie application. The transcript assembly of each sample sorted by the StringTie (v2.1.3b) program was prepared using the reference annotation file (Sus scrofa Sscrofa 11.1.99). The GTF files of each obtained sample were merged and compared through the gffcompare program (v 0.11.6) and converted through the gffread (v 0.11.8). For the screening of potential novel lncRNAs, those with transcript lengths longer than 200 bp and those with class codes "I", "j", "o", "u", and "x" were selected. TransDecoder (v5.5.0) was used to determine the transcripts with an open reading frame (ORF) length of less than 300 bp. Furthermore, Coding Potential Calculator2 (CPC2), predictor of lncRNAs and messenger RNAs based on an improved k-mer scheme (PLEK) v1.2, RNA coding potential assessment tool (CPAT) v1.2.4, and Coding-Non-Coding Index (CNCI) were used to predict the coding potential of the remaining transcripts. Transcripts with a high probability of non-coding were selected using information from the protein families (PFAM) v33.0 and the RNA families (RFAM) v14.2 databases. The HMMER program (v3.3) was used to filter the known protein family domain, and the internal program (v1.1.2) was used to filter housekeeping RNAs. Transcripts presumed to be potential lncRNAs were removed in only 1 out of 68 samples (ovary, oviduct, endometrium). The processes used to identify novel lncRNAs are illustrated in Fig. 2A.

Characteristics of putative lncRNAs

Various genomic characteristics were identified to confirm the specific properties of the newly obtained lncRNA. The number of exons, transcript length, and genomic location were determined through a final combined GTF file (Fig. 2A). Since tissue specificity is a notable feature of lncRNA, the tissue specificity index (TSI) of lncRNA was calculated. The lncRNAs used included the novel lncRNAs and known lncRNAs. The TSI is calculated as follows:

$$TSI = \frac{\sum_{i=1}^{N}(1 - x_i)}{N - 1},$$

where N is the number of tissues, and x_i is the fragment per kilobase of exon per million mapped fragments (FPKM) value of lncRNA/mRNA x in tissue i normalized by the maximum value of FPKM [35].

Overall expression levels of lncRNA and mRNA genes

The expression patterns were obtained to determine tissue-specific and timepoint-specific lncRNAs and mRNAs according to the estrous cycle. The trimmed mean of M (TMM) value was used to normalize raw counts and estimate the expression levels of lncRNAs and mRNAs. Differential expression analyses were performed at each time point (D03, D06, D09, D12, D15, and D18) and compared with those at D00 for each tissue (ovary, oviduct, and endometrium) by using the R package (edge R 3.32.1); an absolute $\log_2$ fold-change (FC) of≥ 1 and false discovery rate (FDR) of < 0.05 were used as cutoff criteria for differentially expressed (DE) lncRNAs and mRNAs. A multidimensional scaling (MDS) plot and a volcano plot of DE lncRNAs and mRNAs were

https://doi.org/10.5187/jast.2023.e137

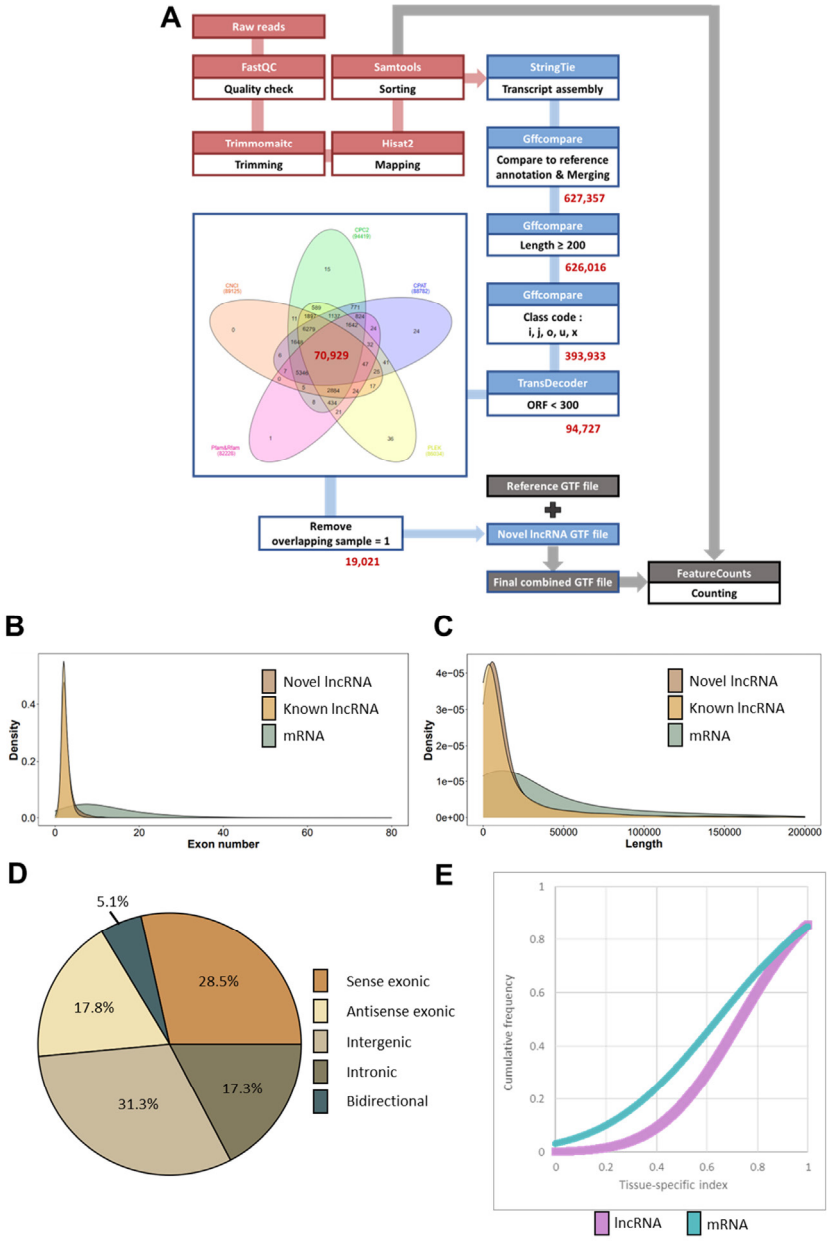

Fig. 2. Acquisition and genomic characterization of the novel lncRNA. (A) Filtering and number of novel lncRNA. (B) Comparison of the distribution of the exon number between lncRNAs (novel lncRNAs and known lncRNAs) and mRNAs. (C) Comparison of the distribution of the transcript length between lncRNAs (novel lncRNAs and known lncRNAs) and mRNAs. (D) Classification of novel lncRNAs. Percentage of exonic, intergenic, intronic, and bidirectional regions. (E) Comparison of the tissue-specific index (TSI) of lncRNA and mRNA. The cumulative distribution of TSI of lncRNAs (novel lncRNAs and known lncRNAs) and mRNAs. ORF, open reading frames; lncRNA, long non-coding RNA.

drawn by ggplot2 and limma function of the R package.

Network construction of lncRNAs

Network analysis was conducted via weighted gene co-expression network analysis (WGCNA) package in R to examine their correlation between lncRNAs and phenotypes (tissue and time

specific according to the estrous cycle and hormonal changes). Hormone-related traits consisting of steroid hormones (follicle-stimulating hormone [FSH], luteinizing hormone [LH], P4, E2, inhibin) that play important roles in the estrous cycle [11]. Hormone data were measured from blood samples at seven time points (D00, D03, 06, D09, D12, D15, and D18) over the estrous cycle, and detailed methods and explanations are described in the paper [36]. The content of these hormonal traits is summarized in Supplementary Table S1. Correlations were calculated on the basis of co-expression, and the module (network) with high correlation was constructed using the $\log_2$TMM value of lncRNA. In the case of hormone traits, the data corresponding to each estrous cycle at seven time points were analyzed for correlation and expressed as a correlation coefficient. Among the modules, three tissue-specific modules (ovary, oviduct, endometrium specific) and one hormone-specific module were selected. Network visualization was performed using the Cytoscape (v3.8.2) software.

Cis-nearby targeted DEmRNAs of lncRNAs

Cis-acting genes were confirmed from the main lncRNAs in four networks. *Cis*-regulatory elements or *cis*-regulatory modules are noncoding DNA regions that regulate the transcription of neighboring genes [37]. In *cis*, lncRNA regulates nearby sequences in the genome, and various related results confirmed that such lncRNAs are found within 100 kb of transcriptional regulation-related coding genes [37]. Therefore, coding genes were searched within 100 kb upstream and downstream of the main lncRNA because the *cis*-activity of lncRNA is related to interaction with adjacent target genes [35,38]. The expression patterns of lncRNAs and their *cis*-acting genes of each network in tissues and time point were confirmed using Multi Experiment Viewer (MeV v4.9.0) by the k-means clustering algorithm. The number of the main lncRNAs and main DE lncRNAs was shown as a circos plot; their *cis*-acting genes and DE *cis*-acting genes were determined using the circa program (v1.2.1).

Functional analyses

Database for annotation, visualization, and integrated discovery (DAVID) 2021 was used to annotate the gene ontology (GO) term and the Kyoto Encyclopedia of Genes and Genomes (KEGG) pathways by using the DE *cis*-acting gene of lncRNAs in the four networks. The ClueGo (v2.5.7) plugin of Cytoscape (v3.8.2) was used to visualize GO terms and KEGG pathways. A pie chart was drawn for the path that met the threshold value of $p < 0.05$, and the KEGG pathways were visualized as a bar graph with $-\log_{10} p$-value and fold enrichment.

RESULTS

Data processing

The RNA-seq reads were generated at seven time points during the estrous cycle in three tissues (ovary, oviduct, and endometrium; Fig. 1) [6]. In 67 tissue samples (from three tissues), 1.3 billion sequence reads were produced with an average of 19.5 million per sample (Supplementary Table S2). The average number of the clean reads after trimming was 1.1 billion sequence reads. The average unique mapping rate (93.93%) and the average overall mapping rate (97.81%) were determined. The MDS results based on transcriptomes (lncRNA and mRNA) showed that the clusters clearly separated for each tissue were common in lncRNAs and mRNAs (Supplementary Fig. S1).

https://doi.org/10.5187/jast.2023.e137

Identification of novel lncRNA

After 627,357 transcripts were obtained through assembly and merging, 626,016 transcripts remained except for those less than 200 bp in length. After the class codes (i, j, o, u, x) of the candidate lncRNA were extracted, 393,933 transcripts remained; of these transcripts, 94,727 had an ORF length of less than 300 bp. Then, 70,929 transcripts were derived using four coding potential assessment tools and two databases; finally, 19,021 novel lncRNA transcripts, excluding the transcripts identified in only one sample (Fig. 2A, Supplementary Table S3), were obtained.

Characteristics of lncRNA

Various types of information about the predicted lncRNA were first investigated and then compared with those of mRNA to determine the genomic characteristics of the acquired novel lncRNA. The average exon number of novel lncRNAs was 2.4, the known lncRNAs was 2.8, and the protein-coding mRNA was 12.3, indicating that lncRNAs tended to be less than mRNAs (Fig. 2B). The mean transcript length of the novel ncRNA was about 18,763 bp, the known lncRNA was about 22,846 bp, and the protein-coding mRNA was about 56,276 bp. The transcript length also showed that lncRNAs tend to be shorter than mRNAs (Fig. 2C), which were consistent with previous studies [39,40]. In addition, the transcript location of the novel lncRNA was classified as follows: 31.3% of intergenic regions that did not overlap with the protein-coding gene, 17.3% of intronic, 28.5% of sense exonic, 17.8% of antisense exonic, and 5.1% bidirectional (Fig. 2D). Finally, the TSI was calculated to determine the tissue specificity of lncRNAs. Similar to previous results [29], the average TSI (0.73) of lncRNAs was higher than the average TSI (0.64) of mRNAs (Fig. 2E).

Differential expression of lncRNA and mRNA

The differential expression levels of lncRNAs and mRNAs in each of the three reproductive tissues (ovary, oviduct, and endometrium) were investigated at six time points (D03, D06, D09, D12, D15, and D18) based on the estrous cycle D00 (Fig. 1). The patterns of changes in the upregulated and downregulated expression levels of lncRNA and mRNA for each tissue were similar (Supplementary Fig. S2). The number of DE transcripts in the ovary gradually decreased until D18 after many differential expression levels were observed on D06 and D09. The number of DE transcripts in the endometrium also increased until D09 and then gradually decreased. In the oviduct, DE transcripts increased until D12 and decreased thereafter; the smallest number of DE transcripts was also found in the oviduct (Supplementary Fig. S3). In addition, the number of overlapping DE lncRNAs in the three tissues at each time point was relatively smaller than that of DE mRNA (Supplementary Fig. S4). The list and significant values of all DE lncRNAs and mRNAs are summarized in Supplementary Table S4.

Co-expression network of lncRNA

Six modules (networks) of lncRNAs that correlated with hormones, reproductive tissues, and time points were calculated (Supplementary Fig. S5). Among them, four modules (blue, green, red, and yellow) were set to represent high significance with traits. Blue, green, and red modules were highly correlated in each of the three tissues (ovary, oviduct, and endometrium), and the yellow module was correlated with changes in each hormone (Fig. 3A). The blue, green, red, and yellow modules had 3,243, 2,725, 2,682, and 24 lncRNAs, respectively, and four co-expression networks were generated using the WGCNA from these four modules. The blue network, which showed an ovary tissue-specific correlation, consisted of 130 nodes (lncRNAs) and 234 edges (interactions); it also had the largest number of nodes (Fig. 3B). The green network, which showed oviduct tissue-specific correlation, comprised 45 nodes and 181 edges (Fig. 3C). The red network, which exhibited

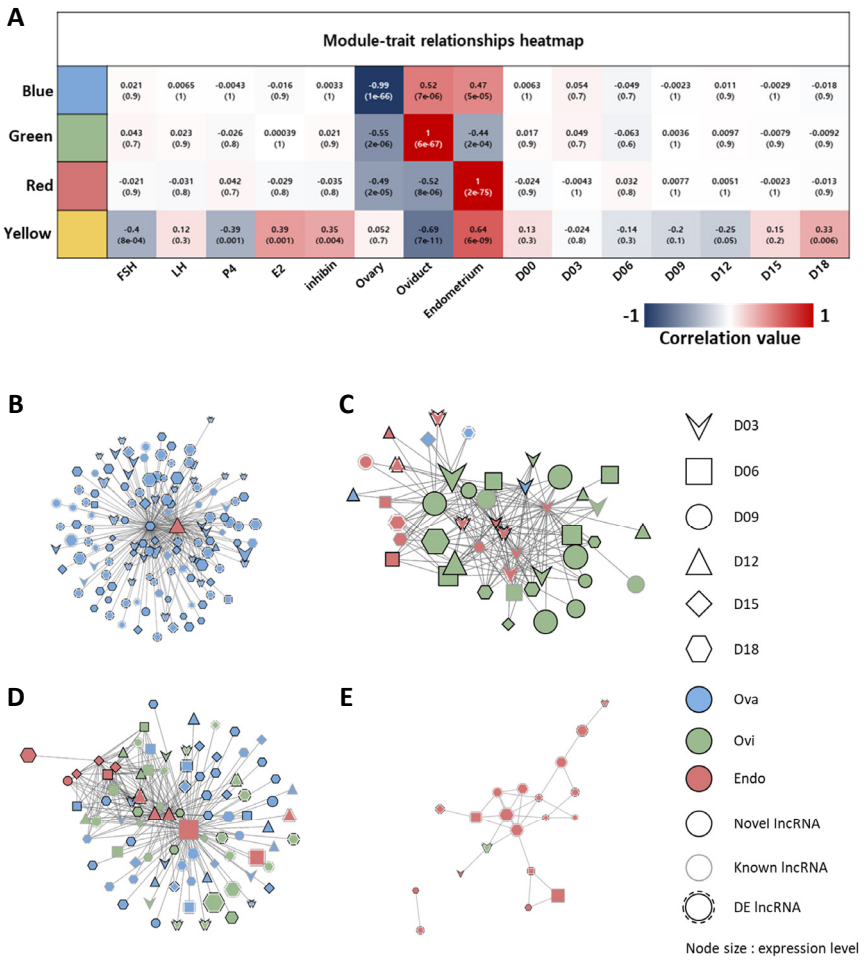

Fig. 3. Network analysis of lncRNA based on the heatmap of four module–trait relationships. Node color indicates three tissues, node size corresponds to the expression level, and node shape refers to the six time points (D03, V shape; D06, rectangle; D09, ellipse; D12, triangle; D15, diamond; D18, hexagon). The border of the node indicates the types of lncRNA (novel lncRNA, black line; known lncRNA, gray line; DE lncRNA: parallel line). The red star refers to the core lncRNA. (A) Heatmap of four module–trait relationships of lncRNA according to hormones, tissues (ovary, oviduct, endometrium), and days (D00, D03, D06, D09, D12, D15, D18). (B) Correlation network of lncRNAs in the blue module. The lncRNA marked with a red star is XLOC_000748. (C) Correlation network of lncRNAs in the green module. (D) Correlation network of lncRNAs in the red module. The lncRNA marked with a red star is ENSSSCG00000051124. (E) Correlation network of lncRNAs in the yellow module. Ova, ovary; Ovi, oviduct; Endo, endometrium; lncRNA, long non-coding RNA.

endometrium tissue-specific correlation, consisted of 93 nodes 265 edges (Fig. 3D). The yellow network, which indicated the correlation with hormones, had 20 nodes 30 edges (Fig. 3E). Among the lncRNAs constituting the network, DE lncRNA had the highest number of 70 in the blue network and the smallest number of 8 in the green network; furthermore, 27 and 16 DE lncRNAs were found in the red and yellow networks, respectively.

Cis-acting gene profiling based on the main lncRNA

The *cis*-acting gene of each lncRNA was searched to identify the coding genes regulated by the main lncRNAs in the network [37]. These lncRNAs and *cis*-acting genes were distributed in all chromosomes except chromosome 7, and relatively many *cis*-acting genes were found in the blue and red networks in proportion to the number of lncRNAs (Fig. 4). Furthermore, 240 *cis*-acting

https://doi.org/10.5187/jast.2023.e137

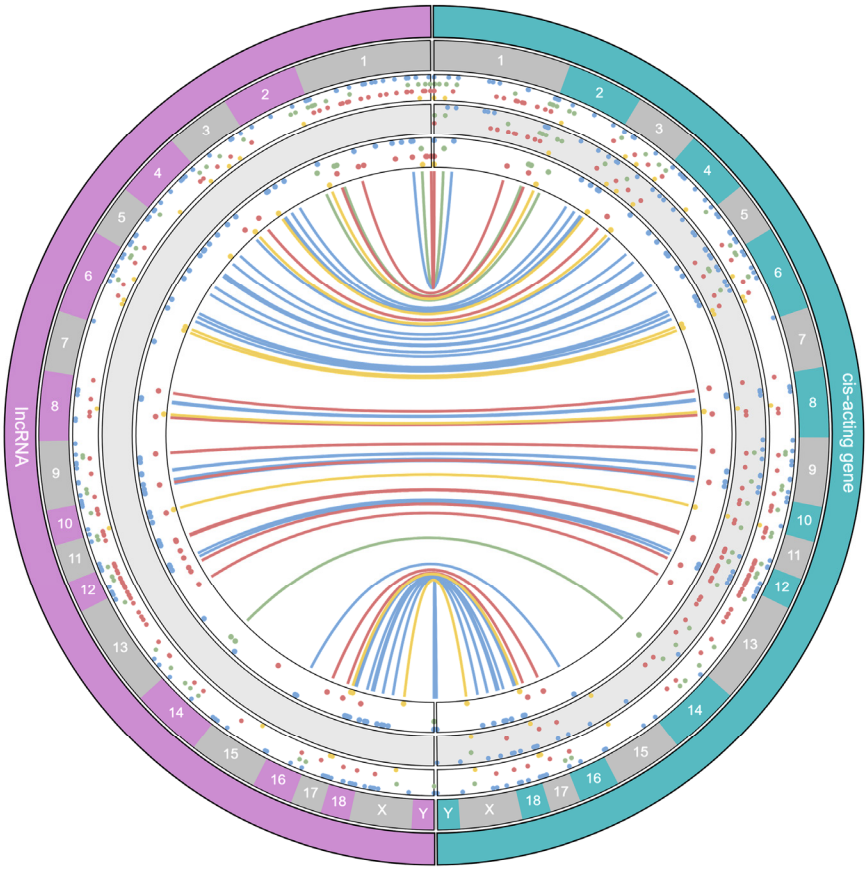

Fig. 4. Distribution of lncRNA and the cis-acting gene for each network in different chromosomes. The outer layer of the lncRNA category indicates the lncRNA included in the network for each module, and the inner layer contains only DE lncRNAs among them. The outer layer of the *cis*-acting gene category refers to the *cis*-acting gene of lncRNAs included in the network for each module, the middle layer contains only DE *cis*-acting gene from the outer layer, and the innermost layer contains only the *cis*-acting gene of DE lncRNA in the middle layer. The innermost circle shows the linkage between the DE lncRNA of each network and their DE *cis*-acting gene. lncRNA, long non-coding RNA; DE, differentially expressed.

genes were identified from 130 lncRNAs in the blue network, 152 *cis*-acting genes were identified from 45 lncRNAs in the green network, 262 *cis*-acting genes were identified from 93 lncRNAs in the red network, and 48 *cis*-acting genes were identified from 20 lncRNAs in the yellow network, which were visualized in the outer layer. Among the *cis*-acting genes searched in this way, 105 in blue networks, 56 in green networks, 112 in red networks, and 18 in yellow networks were DE, and they were shown in the middle layer of the *cis*-acting gene category. Among them, the DE *cis*-acting genes of DE lncRNAs in each network were found in the inner layer, with 48 blue networks, 13 green networks, 31 red networks, and 14 yellow networks. The *cis* interactions between them and the main DElncRNA were visualized as a line in the innermost circle. A list of lncRNAs and *cis*-acting genes is presented in Supplementary Table S5.

Functional annotations

Naturally, lncRNAs with a *cis*-acting mechanism have low expression levels, and they have the potential to regulate mRNAs even with such a low expression [37]. Therefore, functional analysis was performed with the genes in the middle layer of the *cis*-acting gene category in Fig. 4. First,

the expression patterns of DE *cis*-acting genes and lncRNAs interacting with one another were compared. In each of the three tissue-specific networks, two expression patterns were determined: a cluster in which the expression patterns of the two groups of genes were directly proportional and another cluster in which the expression patterns of the two groups of genes were inversely proportional to the ovarian tissue (Supplementary Figs. S6A, S6B, and S6C). In addition, in the hormone-specific network, the two gene groups were distinguished with two expression patterns: a cluster that was directly proportional to the whole tissue and a cluster that was inversely proportional to the whole tissue (Supplementary Fig. S6D).

From the DE *cis*-acting genes corresponding to the blue module network, the KEGG pathways (neuroactive ligand-receptor interaction, ubiquitin mediated proteolysis, etc.) and BP terms (regulation of ion transmembrane transport, protein polyubiquitination, etc.) were enriched (Fig. 5A). From the DE *cis*-acting genes corresponding to the green module network, the KEGG pathways (tight junction, thyroid hormone synthesis, etc.) and BP terms (positive regulation of MAP kinase activity, positive regulation of cell migration, epithelial cell morphogenesis, toxin

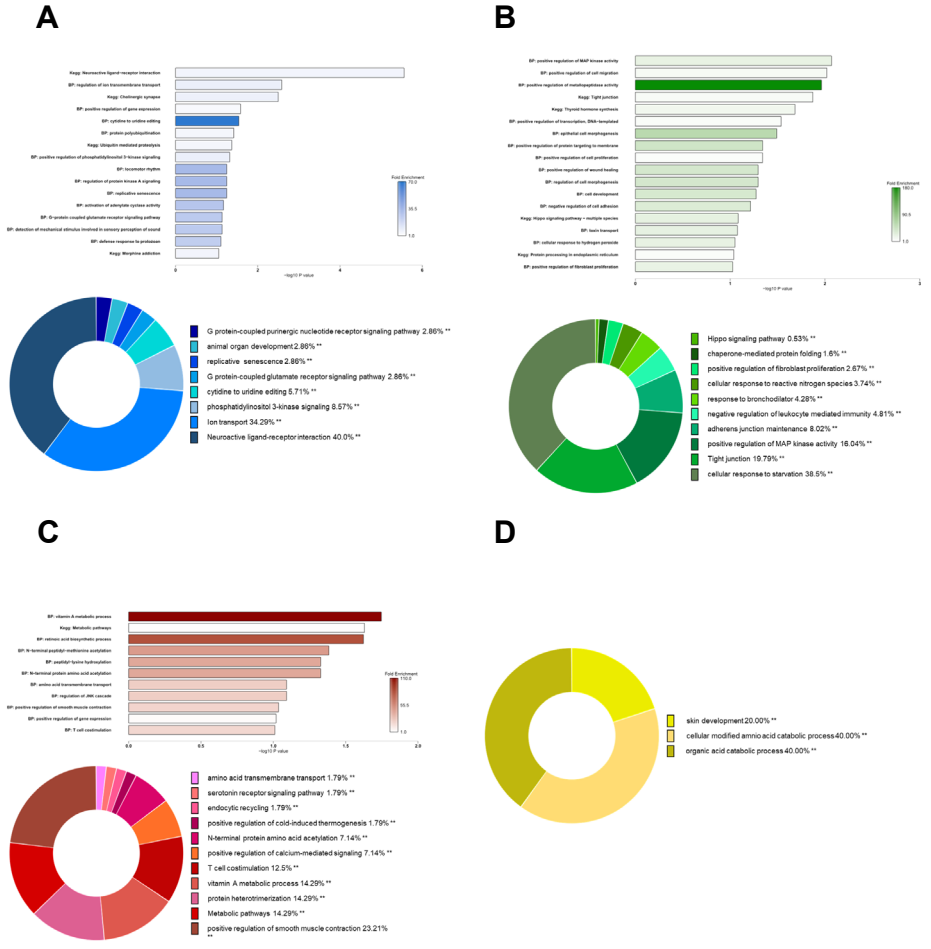

Fig. 5. Visualization of the functional analyses of DE *cis*-acting gene of lncRNAs included in the network for each module. Bar graph of biological process (BP) and Kyoto Encyclopedia of Genes and Genomes (KEGG) pathways using DAVID analysis. Pie chart of BP term and KEGG pathways via Cytoscape (**$p < 0.05$). (A) Bar graph and pie chart of the correlation network of lncRNAs in the blue, (B) green, and (C) red modules. (D) Pie chart of the correlation network of lncRNAs in the yellow module. DE, differentially expressed; lncRNA, long non-coding RNA.

https://doi.org/10.5187/jast.2023.e137

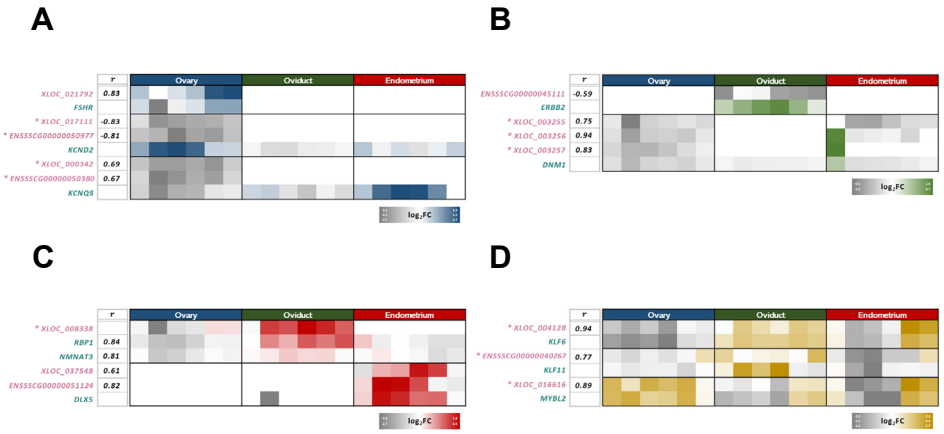

Fig. 6. Correlation heatmap of the main lncRNA and *cis*-acting gene. Correlation coefficients (*r*) were calculated as log_2FC values. Log_2FC of D03, D06, D09, D12, D15, and D18 in order from the first column to the last column of each tissue category. LncRNAs marked with an asterisk (*) indicate DElncRNAs. (A) Correlation heatmap of the main lncRNA and cis-acting gene of the network from the blue, (B) green, (C) red, and (D) yellow modules. DElncRNA, differentially expressed long non-coding RNA.

transport, etc.) were enriched (Fig. 5B). From the DE*cis*-acting genes corresponding to the red module network, the KEGG pathway (metabolic pathways) and BP terms (vitamin A metabolic process, retinoic acid biosynthesis, N-terminal protein amino acid acetylation, T cell costimulation, etc.) were enriched (Fig. 5C). From the DE *cis*-acting genes corresponding to the yellow module network, BP terms (skin development, cellular-modified amnio acid catabolic process, organic acid catabolic process, etc.) were enriched (Fig. 5D). The detailed information on enriched genes and their significant values are summarized in Supplementary Table S6.

FSHR, *KCND2*, and *KCNQ5* were the main *cis*-acing genes involved in functional analysis of the lncRNAs of the blue module network, and the lncRNAs with a *cis*-acting relationship were identified to be XLOC_021792, XLOC_017111, ENSSSCG00000050977, XLOC_000342, and ENSSSCG00000050380 (Fig. 6A). The main *cis*-acing genes involved in the functional analysis of the genes of the green module network were *ERBB2* and *DNM1*; ENSSSCG00000045111, XLOC_003255, XLOC_003256, and XLOC_003257 were the lncRNAs having a *cis*-acting relationship with them (Fig. 6B). *RBP1*, *NMNAT3*, and *DLX5* were the main *cis*-acing genes involved in the functional analysis of the genes of the red module network, and XLOC_008338, XLOC_037548, and ENSSSCG00000051124 were the lncRNAs showing a *cis*-acting relationship with them (Fig. 6C). *KLF6*, *KLF11*, and *MYBL2* were the main *cis*-acing genes involved in the functional analysis of the genes of the yellow module network; XLOC_004128, ENSSSCG00000040267, and XLOC_016616 were the lncRNAs having a *cis*-acting relationship with them (Fig. 6D).

DISCUSSION

Dynamic changes in lncRNAs during the estrous cycle

Swine reproductive tissues undergo various tissue-integrated and tissue-specific changes during the estrous cycle. During the proestrus period (D16–D21), FSH is secreted by GnRH in preparation for estrus, and estrogen secretion increases as the follicle matures for ovulation [9]. At this time, E2, an estrogen steroid hormone, thickens the lining of the uterus to create an environment where a follicle can be implanted when the follicle is fertilized [41]. After the peak of E2 and FSH secretion

in the estrus period (D00–D03), fully mature follicles become ovulated [9]. In the metestrus period (D04–D06), luteinization begins, P4 secretion begins, and the follicle from the oviduct is released [17]. In diestrus (D07–D15), which is the longest phase of the estrus cycle, the corpus luteum continues to develop in the ovary, and P4 secretion increases continuously [9]. P4 helps keep the endometrium fertile and stimulates PGF2α secretion by the endometrium [42–44]. If pregnancy is not achieved until approximately D15, PGF2α is secreted from the endometrium to the ovary, and the corpus luteum is degenerated to reduce P4 secretion, contract the uterus, and return to the proestrus state [45,46]. With these changes, the mRNA expression undergoes tissue-integrated and tissue-specific changes during the estrous cycle [6]. The lncRNA expression also changes, and its expression pattern is similar to that of mRNA (Supplementary Figs. S2 and S3). This finding suggests that mRNAs and lncRNAs are involved in the changes in three reproductive tissues during the estrous cycle. In this study, WGCNA analysis was performed to determine the correlation between these lncRNAs. Among the modules constructed through lncRNA co-expression analysis, the tissue-specific lncRNAs of three reproductive tissues during the estrous cycle were investigated using three modules, and tissue-integrated lncRNAs were examined by identifying hormonal changes in the three tissues using one module. These generated modules revealed the existence of lncRNAs specifically regulated by tissue or hormonal changes.

Development of each tissue by the main lncRNA and cis-acting gene

First, the tissue-specific lncRNAs of the ovary were obtained from the network constructed through the blue module (Fig. 3B). BP terms and KEGG pathway enrichment analyses were performed to reveal the association between the molecular function of the corresponding DE *cis*-acting gene of lncRNAs and the estrous cycle. Numerous main terms essential for ovarian development and function were identified (Fig. 5A).

Among the lncRNA and *cis*-acting gene pairs involved in these functions, five pairs had significant expression patterns and correlations (Fig. 6A). Previous studies confirmed that the neuroactive ligand-receptor interaction pathway may play an important role in follicle production and ovarian function regulation in poultry and fish; it may also influence steroid hormone synthesis in the gonads [47]. *FSHR* is highly expressed in ovarian granulosa cells; it is a key gene involved in ovarian function and stimulated primarily by FSH to regulate follicle growth and maturation, as well as estrogen production [48]. In our study, *FSHR* and XLOC_021792 were highly expressed when FSH was the most secreted for ovulation (D16–D03); therefore, a novel lncRNA, namely, XLOC_021792, could positively regulate *FSHR* through a *cis*-acting relationship (Fig. 6A). In addition, ovarian follicles have a characteristic pattern of bioelectrical activity and ion transport mechanisms; they are also involved in a range of oogenesis through Na^+, K^+, and Cl^- channel activation and ion transport [49,50]. Among the K^+ genes, *KCND2*, which acts as a steroid sensor and generates bioelectrical signals for follicle production, and *KCNQ5* from the KCNQ family, which is an important substance in ion channels in hamster ovarian cells, were identified in our sample [51,52]. Our results showed that *KCND2* could be negatively regulated as a *cis*-acting relationship from novel lncRNA XLOC_017111 and known lncRNA ENSSSCG00000050977; *KCNQ5* was positively regulated as a *cis*-acting relationship from novel lncRNA XLOC_000342 and the known lncRNA ENSSSCG00000050380 (Fig. 6A). Since the period of the high KNCD2 expression (D7–D15), which acts as a steroid sensor, was very similar to the period of progesterone secretion in the corpus luteum, XLOC_017111 and ENSSSCG00000050977, which were negatively regulated in the *cis*-acting relationship, would affect progesterone secretion.

Tissue-specific lncRNAs of the oviduct were obtained from the network constructed through the green module (Fig. 3C). BP terms and KEGG pathways related to cell morphogenesis and cell

https://doi.org/10.5187/jast.2023.e137

development in oviductal tissues were identified from the DE *cis*-acting genes of these lncRNAs (Fig. 5B). Among the lncRNA and *cis*-acting gene pairs involved in these functions, four pairs had significant expression patterns and correlations (Fig. 6B). In the porcine oviductal tissue, MAP kinase activity stimulates gene expression and cell division; it also favors the formation of epithelial cells of the fallopian tubes and prevents the entry of toxic materials or pathogens by controlling permeability via tight junctions [53–55]. *ERBB2*, which is involved in both of these key terms and in epithelial cell development and signaling [56], is negatively regulated in a *cis*-acting relationship by ENSSSCG00000045111, a known lncRNA (Fig. 6B). In the period of high *ERBB2* expression (D04–D15), the follicle moves to the uterus through the oviduct after ovulation to prepare for pregnancy. ENSSSCG00000045111 was likely involved in the formation of tubal epithelial tissue during this period.

The tissue-specific lncRNAs of the endometrium were obtained from the network constructed through the red module (Fig. 3D). The main terms related to uterine development for embryo implantation were identified from the DE *cis*-acting genes of these lncRNAs (Fig. 5C). Among the lncRNA and *cis*-acting gene pairs involved in these functions, four pairs had significant expression patterns and correlations (Fig. 6C). Retinol (vitamin A) and retinol-binding protein (RBP) secreted into the endometrium were implicated in the development of the porcine endometrium and embryonic formation. These RBPs participate in the storage, metabolism, and transport of retinol to target cells and in uterine growth and morphogenesis. RBP has four morphological categories that affect the endometrium in various ways [57–59]. In our study, among RBPs, *RBP1* was positively correlated with XLOC_008338, a novel lncRNA; in comparison with other tissues, when XLOC_008338 was not expressed in the endometrium, the expression of *RBP1* was also suppressed (Fig. 6C). The expression of *RBP1* possibly increased for implantation at the time of ovulation (D03), but the expression of *RBP1* likely decreased because implantation did not occur (D4–D21). At this time, *NMNAT3* had a high positive correlation in the *cis*-acting relationship such as *RBP1* and XLOC_008338, and it was affected by XLOC_008338. *NMNAT3* likely participated in endometrial morphogenesis.

Regulation of the steroid hormone during the estrous cycle by lncRNA

Tissue-integrated lncRNAs were obtained from the yellow module constructed according to the correlation of hormone changes (Fig. 3E). The genes correlated in the *cis*-acting relationship with these lncRNAs in all tissues and estrous cycles were *CHST9*, *DECR2*, *KLF6*, *KLF11*, *MYBL2*, and *PCDH19* (Fig. 6D, Supplementary Fig. S7). The KLF family can be expressed in tissues that respond to steroid hormones in relation to the action of the progesterone receptor (PGR) and estrogen receptor (ESR) [60]. In the present study, *KLF6* and *KLF11* were highly expressed when PGF2α was secreted for ovarian P4 inhibition in the endometrium (D16–D21); thus, P4 was inhibited and E2 was highly expressed in th eovary during secretion. *KLF6* was highly correlated with novel lncRNA XLOC_004128, and *KLF11* was highly correlated with known lncRNA ENSSSCG00000040267; This high correlation seemed to be affected by the *cis*-acting relationship with lncRNAs (Fig. 6D). Therefore, these lncRNAs were likely closely related to the secretion of PGF2α from the endometrium and the secretion of E2 from the ovary. *MYBL2* showed a similar expression pattern in the endometrium and an opposite expression pattern in the ovary. XLOC_016616 also showed an expression pattern similar to that of *MYBL2*, and this expression pattern was possibly regulated in the *cis*-relationship (Fig. 6D). Therefore, XLOC_016616 could be a lncRNA that could affect the secretion of PGF2α from the endometrium and the secretion of P4 from the ovary.

Trans-acting and complex transcriptional participation by lncRNA

The *trans*-acting relationship between lncRNA and coding gene is as important and diverse as the *cis*-acting relationship although it is difficult to verify compared with the *cis*-acting relationship and vague in setting the standard [37]. Usually, the relationship between a lncRNA and a *trans*-acting gene means that they interact even when they are in different chromosomes [61]. In the present study, the core lncRNA was selected through co-expression network construction (Figs. 3B and 3D). Core lncRNAs were highly correlated with the other main lncRNAs in the network present in different chromosomes (Supplementary Fig. S8). Two core lncRNAs, namely, XLOC_000748 and ENSSSCG00000051124, are presented as *trans*-acting lncRNAs. In addition, a coding gene in a *cis*-acting relationship could be affected not only by one lncRNA but also by several lncRNAs. Conversely, one lncRNA may affect multiple genes in a *cis*-acting relationship [37]. In the present study, XLOC_003255, XLOC_008338, XLOC_037548, and other lncRNAs had this potential (Figs. 6A, 6B and 6C). The principle that lncRNA regulates a gene as a *trans*-acting factor and various transcriptional regulation methods of lncRNA are complex and diverse. Consequently, a more complete reference, including the results of this study, should be established to accurately determine how lncRNA plays these roles, and in-depth research based on structural analysis should be performed.

CONCLUSION

In this study, lncRNA (novel lncRNA and known lncRNA) and mRNA expressed during the swine estrous cycle were discovered in three reproductive tissues of pigs, and their expression patterns were similar. Network analysis was performed to analyze the function of lncRNA according to its expression pattern, and *cis*-acting genes were searched to understand the interaction between lncRNA and mRNA. The main lncRNA and *cis*-acting gene significantly expressed according to the estrous cycle in a tissue-specific or tissue-integrated manner were found, and their functions were presented. The expression of these lncRNA and *cis*-acitng gene could be highly related to hormonal activities secreted by each tissue. In the ovary, XLOC_021792 likely regulated FSH secretion during the follicular phase; XLOC_01711, ENSSSCG00000050977, XLOC_000342, and ENSSSCG00000050380 possibly regulated P4 secretion during the luteal phase. ENSSSCG00000045111 controlled the oviductal morphogenesis for pregnancy preparation during the luteal phase, and XLOC_008338 modulated the uterine morphogenesis in the estrus phase. XLOC_004128 and ENSSSCG00000040267 likely inhibited P4 secretion and activated E2 secretion in the ovary during the luteal phase. They were also related to the secretion of PGF2α from the endometrium during the proestrus period. XLOC_016616 was also presented to be a similar lncRNA. These results revealed the possible lncRNAs and their functions that have not been identified in porcine reproductive tissues according to the estrus cycle. Furthermore, this study could help elucidate the activities and interactions of reproductive tissues that were difficult to understand only when mRNA was used as a reference. This study also provided a basis for further research on the specific mechanism by which lncRNA regulates mRNA according to the structure and location of a given lncRNA sequence.

SUPPLEMENTARY MATERIALS

Supplementary materials are only available online from: https://doi.org/10.5187/jast.2023.e137.

https://doi.org/10.5187/jast.2023.e137

REFERENCES

1. Revelle TJ, Robison OW. An explanation for the low heritability of litter size in swine. J Anim Sci. 1973;37:668-75. https://doi.org/10.2527/jas1973.373668x
2. Sharpe RM, Franks S. Environment, lifestyle and infertility — an inter-generational issue. Nat Med. 2002;8:S33-40. https://doi.org/10.1038/nm-fertilityS33
3. Cole DJA. Nutritional strategies to optimize reproduction in pigs. J Reprod Fertil. 1990;Suppl 40:67-82.
4. Li PH, Ma X, Zhang YQ, Zhang Q, Huang RH. Progress in the physiological and genetic mechanisms underlying the high prolificacy of the Erhualian pig. Yi Chuan-Hereditas. 2017;39:1016-24.
5. Zhang F, Tang L, Ran X, Mao N, Ruan Y, Yi F, et al. Changes in ovary transcriptome and alternative splicing at estrus from Xiang pigs with large and small litter size. bioRxiv 547810 [Preprint]. 2019 [cited 2023 Oct 12]. https://doi.org/10.1101/547810
6. Kim JM, Park JE, Yoo I, Han J, Kim N, Lim WJ, et al. Integrated transcriptomes throughout swine oestrous cycle reveal dynamic changes in reproductive tissues interacting networks. Sci Rep. 2018;8:5436. https://doi.org/10.1038/s41598-018-23655-1
7. Liu Y, Li M, Bo X, Li T, Ma L, Zhai T, et al. Systematic analysis of long non-coding RNAs and mRNAs in the ovaries of Duroc pigs during different follicular stages using RNA sequencing. Int J Mol Sci. 2018;19:1722. https://doi.org/10.3390/ijms19061722
8. Ross JW, Ashworth MD, Mathew D, Reagan P, Ritchey JW, Hayashi K, et al. Activation of the transcription factor, nuclear factor kappa-B, during the estrous cycle and early pregnancy in the pig. Reprod Biol Endocrinol. 2010;8:39. https://doi.org/10.1186/1477-7827-8-39
9. Soede NM, Langendijk P, Kemp B. Reproductive cycles in pigs. Anim Reprod Sci. 2011;124:251-8. https://doi.org/10.1016/j.anireprosci.2011.02.025
10. Edson MA, Nagaraja AK, Matzuk MM. The mammalian ovary from genesis to revelation. Endocr Rev. 2009;30:624-712. https://doi.org/10.1210/er.2009-0012
11. Noguchi M, Yoshioka K, Itoh S, Suzuki C, Arai S, Wada Y, et al. Peripheral concentrations of inhibin A, ovarian steroids, and gonadotropins associated with follicular development throughout the estrous cycle of the sow. Reproduction. 2010;139:153-61. https://doi.org/10.1530/REP-09-0018
12. Leese HJ. The formation and function of oviduct fluid. J Reprod Fertil. 1988;82:843-56. https://doi.org/10.1530/jrf.0.0820843
13. Akison LK, Boden Mj, Kennaway DJ, Russell DL, Robker RL. Progesterone receptor-dependent regulation of genes in the oviducts of female mice. Physiol Genomics. 2014;46:583-92. https://doi.org/10.1152/physiolgenomics.00044.2014
14. Wang Y, Xue S, Liu X, Liu H, Hu T, Qiu X, et al. Analyses of Long Non-Coding RNA and mRNA profiling using RNA sequencing during the pre-implantation phases in pig endometrium. Sci Rep. 2016;6:20238. https://doi.org/10.1038/srep20238
15. Hunter RHF, Cook B, Poyser NL. Regulation of oviduct function in pigs by local transfer of ovarian steroids and prostaglandins: a mechanism to influence sperm transport. Eur J Obstet Gynecol Reprod Biol. 1983;14:225-32. https://doi.org/10.1016/0028-2243(83)90264-2
16. Park Y, Park YB, Lim SW, Lim B, Kim JM. Time series ovarian transcriptome analyses of the porcine estrous cycle reveals gene expression changes during steroid metabolism and corpus luteum development. Animals. 2022;12:376. https://doi.org/10.3390/ani12030376
17. Jang MJ, Lim C, Lim B, Kim JM. Integrated multiple transcriptomes in oviductal tissue across the porcine estrous cycle reveal functional roles in oocyte maturation and transport. J Anim Sci.

2022;100:skab364. https://doi.org/10.1093/jas/skab364
18. Ma L, Bajic VB, Zhang Z. On the classification of long non-coding RNAs. RNA Biol. 2013;10:924-33. https://doi.org/10.4161/rna.24604
19. Leung A, Trac C, Jin W, Lanting L, Akbany A, Sætrom P, et al. Novel long noncoding RNAs are regulated by angiotensin II in vascular smooth muscle cells. Circ Res. 2013;113:266-78. https://doi.org/10.1161/CIRCRESAHA.112.300849
20. Li BJ, Jiang DL, Meng ZN, Zhang Y, Zhu ZX, Lin HR, et al. Genome-wide identification and differentially expression analysis of lncRNAs in tilapia. BMC Genomics. 2018;19:729. https://doi.org/10.1186/s12864-018-5115-x
21. Chen L, Shi G, Chen G, Li J, Li M, Zou C, et al. Transcriptome analysis suggests the roles of long intergenic non-coding RNAs in the growth performance of weaned piglets. Front Genet. 2019;10:196. https://doi.org/10.3389/fgene.2019.00196
22. Sun Q, Hao Q, Prasanth KV. Nuclear long noncoding RNAs: key regulators of gene expression. Trends Genet. 2018;34:142-57. https://doi.org/10.1016/j.tig.2017.11.005
23. Statello L, Guo CJ, Chen LL, Huarte M. Gene regulation by long non-coding RNAs and its biological functions. Nat Rev Mol Cell Biol. 2021;22:96-118. https://doi.org/10.1038/s41580-020-00315-9
24. Kosinska-Selbi B, Mielczarek M, Szyda J. Review: long non-coding RNA in livestock. Animal. 2020;14:2003-13. https://doi.org/10.1017/S1751731120000841
25. Gong Y, Huang HT, Liang Y, Trimarchi T, Aifantis I, Tsirigos A. lncRNA-screen: an interactive platform for computationally screening long non-coding RNAs in large genomics datasets. BMC Genomics. 2017;18:434. https://doi.org/10.1186/s12864-017-3817-0
26. Huarte M. The emerging role of lncRNAs in cancer. Nat Med. 2015;21:1253-61. https://doi.org/10.1038/nm.3981
27. Jiang P, Hou Y, Fu W, Tao X, Luo J, Lu H. Characterization of lncRNAs involved in cold acclimation of zebrafish ZF4 cells. PLOS ONE. 2018;13:e0195468. https://doi.org/10.1371/journal.pone.0195468
28. Li Z, Jiang P, Li J, Peng M, Zhao X, Zhang X, et al. Tumor-derived exosomal lnc-Sox2ot promotes EMT and stemness by acting as a ceRNA in pancreatic ductal adenocarcinoma. Oncogene. 2018;37:3822-38. https://doi.org/10.1038/s41388-018-0237-9
29. Jiang L, Yang Q, Yu J, Liu X, Cai Y, Niu L, et al. Identification and expression analysis of lncRNA in seven organs of Rhinopithecus roxellana. Funct Integr Genomics. 2021;21:543-55. https://doi.org/10.1007/s10142-021-00797-6
30. Zhang Y, Huang X, Liu J, Chen G, Liu C, Zhang S, et al. New insight into long non-coding RNAs associated with bone metastasis of breast cancer based on an integrated analysis. Cancer Cell Int. 2021;21:372. https://doi.org/10.1186/s12935-021-02068-7
31. Wang Y, Hua R, Xue S, Li W, Wu L, Kang T, et al. mRNA/lncRNA expression patterns and the function of fibrinogen-like protein 2 in Meishan pig endometrium during the preimplantation phases. Mol Reprod Dev. 2019;86:354-69. https://doi.org/10.1002/mrd.23109
32. Subramanian I, Verma S, Kumar S, Jere A, Anamika K. Multi-omics data integration, interpretation, and its application. Bioinform Biol Insights. 2020;14:1177932219899051. https://doi.org/10.1177/1177932219899051
33. Quirós PM, Prado MA, Zamboni N, D'Amico D, Williams RW, Finley D, et al. Multi-omics analysis identifies ATF4 as a key regulator of the mitochondrial stress response in mammals. J Cell Biol. 2017;216:2027-45. https://doi.org/10.1083/jcb.201702058
34. Zapparoli E, Briata P, Rossi M, Brondolo L, Bucci G, Gherzi R. Comprehensive multi-omics analysis uncovers a group of TGF-β-regulated genes among lncRNA EPR direct

https://doi.org/10.5187/jast.2023.e137

transcriptional targets. Nucleic Acids Res. 2020;48:9053-66. https://doi.org/10.1093/nar/gkaa628
35. Yanai I, Benjamin H, Shmoish M, Chalifa-Caspi V, Shklar M, Ophir R, et al. Genome-wide midrange transcription profiles reveal expression level relationships in human tissue specification. Bioinformatics. 2005;21:650-9. https://doi.org/10.1093/bioinformatics/bti042
36. Knox RV, Vatzias G, Naber CH, Zimmerman DR. Plasma gonadotropins and ovarian hormones during the estrous cycle in high compared to low ovulation rate gilts. J Anim Sci. 2003;81:249-60. https://doi.org/10.2527/2003.811249x
37. Gil N, Ulitsky I. Regulation of gene expression by cis-acting long non-coding RNAs. Nat Rev Genet. 2020;21:102-17. https://doi.org/10.1038/s41576-019-0184-5
38. Kumar H, Srikanth K, Park W, Lee SH, Choi BH, Kim H, et al. Transcriptome analysis to identify long non coding RNA (lncRNA) and characterize their functional role in back fat tissue of pig. Gene. 2019;703:71-82. https://doi.org/10.1016/j.gene.2019.04.014
39. Gong Y, He J, Li B, Xiao Y, Zeng Q, Xu K, et al. Integrated analysis of lncRNA and mRNA in subcutaneous adipose tissue of Ningxiang pig. Biology. 2021;10:726. https://doi.org/10.3390/biology10080726
40. Song F, Wang L, Zhu W, Dong Z. Long noncoding RNA and mRNA expression profiles following igf3 knockdown in common carp, Cyprinus carpio. Sci Data. 2019;6:190024. https://doi.org/10.1038/sdata.2019.24
41. Nakamura S, Douchi T, Oki T, Ijuin H, Yamamoto S, Nagata Y. Relationship between sonographic endometrial thickness and progestin-induced withdrawal bleeding. Obstet Gynecol. 1996;87:722-5. https://doi.org/10.1016/0029-7844(96)00016-6
42. Skarzynski DJ, Bogacki M, Kotwica J. Involvement of ovarian steroids in basal and oxytocin-stimulated prostaglandin (PG) F2α secretion by the bovine endometrium in vitro. Theriogenology. 1999;52:385-97. https://doi.org/10.1016/S0093-691X(99)00137-5
43. Zhang Z, Davis DL. Prostaglandin E and F2α secretion by glandular and stromal cells of the pig endometrium in vitro: effects of estradiol-17β, progesterone, and day of pregnancy. Prostaglandins. 1991;42:151-62. https://doi.org/10.1016/0090-6980(91)90074-P
44. Simmen RC, Simmen FA, Hofig A, Farmer SJ, Bazer FW. Hormonal regulation of insulin-like growth factor gene expression in pig uterus. Endocrinology. 1990;127:2166-74. https://doi.org/10.1210/endo-127-5-2166
45. Fortín S, Sayre BL, Lewis GS. Does exogeneous progestogen alter the relationships among PGF2α, 13,14-dihydro-15-keto-PGF2α, progesterone, and estrogens in ovarian-intact ewes around the time of luteolysis? Prostaglandins. 1994;47:171-87. https://doi.org/10.1016/0090-6980(94)90059-0
46. McCracken JA, Glew ME, Scaramuzzp RJ. Corpus luteum regression induced by prostaglandin F2α. J Clin Endocrinol Metab. 1970;30:544-6. https://doi.org/10.1210/jcem-30-4-544
47. Mu R, Yu YY, Gegen T, Wen D, Wang F, Chen Z, et al. Transcriptome analysis of ovary tissues from low- and high-yielding Changshun green-shell laying hens. BMC Genomics. 2021;22:349. https://doi.org/10.1186/s12864-021-07688-x
48. Zhang Y, Ouyang X, You S, Zou H, Shao X, Zhang G, et al. Effect of human amniotic epithelial cells on ovarian function, fertility and ovarian reserve in primary ovarian insufficiency rats and analysis of underlying mechanisms by mRNA sequencing. Am J Transl Res. 2020;12:3234-54.
49. Krüger J, Bohrmann J. Bioelectric patterning during oogenesis: stage-specific distribution of membrane potentials, intracellular pH and ion-transport mechanisms in Drosophila ovarian

follicles. BMC Dev Biol. 2015;15:1. https://doi.org/10.1186/s12861-015-0051-3
50. Fazelkhah A, Braasch K, Afshar S, Salimi E, Butler M, Bridges G, et al. Quantitative model for ion transport and cytoplasm conductivity of chinese hamster ovary cells. Sci Rep. 2018;8:17818. https://doi.org/10.1038/s41598-018-36127-3
51. Mayerhofer A, Kunz L. Ion channels of primate ovarian endocrine cells: identification and functional significance. Expert Rev Endocrinol Metab. 2006;1:549-55. https://doi.org/10.1586/17446651.1.4.549
52. Gamper N, Stockand JD, Shapiro MS. The use of Chinese hamster ovary (CHO) cells in the study of ion channels. J Pharmacol Toxicol Methods. 2005;51:177-85. https://doi.org/10.1016/j.vascn.2004.08.008
53. Wollenhaupt K, Tomek W, Brüssow KP, Tiemann U, Viergutz T, Schneider F, et al. Effects of ovarian steroids and epidermal growth factor (EGF) on expression and bioactivation of specific regulators of transcription and translation in oviductal tissue in pigs. Reproduction. 2002;123:87-96. https://doi.org/10.1530/rep.0.1230087
54. Ariyadi B, Isobe N, Yoshimura Y. Expression of tight junction molecule "claudins" in the lower oviductal segments and their changes with egg-laying phase and gonadal steroid stimulation in hens. Theriogenology. 2013;79:211-8. https://doi.org/10.1016/j.theriogenology.2012.10.018
55. Chen S, Einspanier R, Schoen J. Transepithelial electrical resistance (TEER): a functional parameter to monitor the quality of oviduct epithelial cells cultured on filter supports. Histochem Cell Biol. 2015;144:509-15. https://doi.org/10.1007/s00418-015-1351-1
56. Lim CH, Ahn SE, Lim W, Jeong W, Kim J, Bazer FW, et al. Estrogen regulates ERRFI1 expression during development of the chicken oviduct. In: The 28th Annual General Meeting and Academic Presentation of the Korean Poultry Society; 2011; Cheonan, Korea. p. 121-2.
57. Schweigert FJ, Bonitz K, Siegling C, Buchholz I. Distribution of vitamin A, retinol-binding protein, cellular retinoic acid-binding protein I, and retinoid X receptor β in the porcine uterus during early gestation. Biol Reprod. 1999;61:906-11. https://doi.org/10.1095/biolreprod61.4.906
58. Ma X, Li PH, Zhu MX, He LC, Sui SP, Gao S, et al. Genome-wide association analysis reveals genomic regions on chromosome 13 affecting litter size and candidate genes for uterine horn length in Erhualian pigs. Animal. 2018;12:2453-61. https://doi.org/10.1017/S1751731118000332
59. Chen X, Li A, Chen W, Wei J, Fu J, Wang A. Differential gene expression in uterine endometrium during implantation in pigs. Biol Reprod. 2015;92:52. https://doi.org/10.1095/biolreprod.114.123075
60. Heard ME, Velarde MC, Giudice LC, Simmen FA, Simmen RCM. Krüppel-like factor 13 deficiency in uterine endometrial cells contributes to defective steroid hormone receptor signaling but not lesion establishment in a mouse model of endometriosis. Biol Reprod. 2015;92:140. https://doi.org/10.1095/biolreprod.115.130260
61. Elling R, Robinson EK, Shapleigh B, Liapis SC, Covarrubias S, Katzman S, et al. Genetic models reveal cis and trans immune-regulatory activities for lincRNA-Cox2. Cell Rep. 2018;25:1511-24. https://doi.org/10.1016/j.celrep.2018.10.027

https://doi.org/10.5187/jast.2023.e137